

Living Plant-Hybrid Generators for Multidirectional Wind Energy Conversion

Fabian Meder,* Marc Thielen, Alessio Mondini, Thomas Speck, and Barbara Mazzolai*

The largest existing biological interface, the surface of living plants, as it stands is capable of converting mechanical energy into electricity based on a combination of contact electrification and electrostatic induction on the plant surface and its inner tissue. Herein, the first design strategies are reported for living plant-based wind energy harvesting systems that use this effect and that are capable of harvesting simultaneously from multiple leaves of a single plant to upscale the energy output. This is the first study under outdoor-relevant conditions in a controlled test environment that relates plant-based energy conversion to wind speed and wind direction as well as parameters such as the environmental humidity. Increasing the wind speed not only leads to higher power but also low winds of 2 m s^{-1} and less can be converted into storable electricity. The plant-hybrid generators are moreover capable of converting wind from multiple directions by exploiting the naturally multiplex leaf orientations and the plants can directly power light-emitting diodes (LEDs) and a digital thermometer. The results draw attention to the opportunity to obtain living plant-hybrid generators, e.g., for applications in constituting environmental sensor networks.

1. Introduction

Harvesting energy from the environment and natural resources in a green, carbon-neutral, and resource-saving manner is essential for future energy supplies on large and small scales. In particular, self-powered, wireless sensor networks, and other off-grid microdevices benefit from small autonomous generators, world-wide available without restrictions to stationary power supplies. Bioinspiration is an important driver for technological innovations, and several biohybrid energy harvesting systems are capable of converting chemical and mechanical energy of living entities into electricity.^[1–6] Plants are among the most fascinating organisms that have optimized their own energy supplies including a dynamic self-repair with no more than light, water, carbon dioxide, and (mineral) nutrients.^[7–10] Yet, deriving energy from plants typically requires combusting them


as biomass or biofuels. In another approach, living-plant-hybrid technologies attempt going a step further using living plants in devices to substitute artificial components making use of the specific plant material properties and functionalities.^[11–18] The applications range from plant-based energy harvesting to sensing. The overall approach reduces resources required for the final devices and at once bears the potential for a sustainable technology joining in natural environments.

There are several ways to produce electricity with living plants: plant microbial fuel cells (harvest energy from the living plant root microbiome) and other biophotovoltaic approaches indirectly use photosynthesis,^[19–25] and glucose biofuel cells exploit plant sap's glucose as "fuel".^[26,27] In both examples, the conversion from chemical energy into electricity is done by an artificial fuel cell that uses organic molecules provided by the plant. In contrast, it was recently reported that plants can directly convert mechanical energy into electricity.^[6,28–30] The conversion is based on the coupling of contact electrification and induction of the generated charges into the inner plant tissue enabled by the materials and structure of the outermost tissue layer. All land plants have a largely dielectric outer surface due to a thin polymeric layer covering the surface, named the cuticle. The heterogeneous polymeric phase is produced by the epidermis cells mostly to avoid water evaporation from the inner tissues among other functions.^[31] When brought in mechanical contact with another material, the dielectric cuticle establishes surface charges through contact electrification.^[6,29] It is crucial that

Dr. F. Meder, Dr. A. Mondini, Dr. B. Mazzolai
Istituto Italiano di Tecnologia
Center for Micro-BioRobotics
Viale Rinaldo Piaggio 34, Pontedera, Pisa 56025, Italy
E-mail: fabian.meder@iit.it; barbara.mazzolai@iit.it

Dr. M. Thielen, Prof. T. Speck
Plant Biomechanics Group
Botanic Garden
Faculty of Biology
University of Freiburg
Schänzlestraße 1, Freiburg 79104, Germany

Prof. T. Speck
Cluster of Excellence livMatS
Freiburg Center for Interactive Materials and Bioinspired Technologies (FIT)
University of Freiburg
Georges-Köhler-Allee 105, Freiburg 78110, Germany

 The ORCID identification number(s) for the author(s) of this article can be found under <https://doi.org/10.1002/ente.202000236>.

© 2020 The Authors. Published by WILEY-VCH Verlag GmbH & Co. KGaA, Weinheim. This is an open access article under the terms of the Creative Commons Attribution License, which permits use, distribution and reproduction in any medium, provided the original work is properly cited.

The copyright line for this article was changed on May 19th after original online publication.

DOI: 10.1002/ente.202000236

the dielectric cuticle in living plants is coupled to the ion-conductive cellular tissue forming a dielectric-conductor double layer. The charges generated on the cuticle are electrostatically induced into the conductive tissue leading to a current that can be harvested by an electrode in the plant tissue. The mechanism is principally the same as that exploited in triboelectric generators made of artificial materials and they are considered a possible energy source for the Internet of things and wearable electronics with reported power densities up to several hundred watts per meter square.^[32–34] Applications in agricultural sectors are hypothetical, e.g., recently a microplasma discharge from an artificial triboelectric generator has been used for nitrogen fixation producing a plant fertilizer.^[35] Interestingly, although these artificial generators are in their origin not bioinspired, living plants establish these structures and it remains to be investigated if the organism actively uses it, e.g., for sensing or other processes.^[6] All land plants are principally able to perform energy conversion in this manner as they share the same basic double-layer material structure of dielectric cuticle and ion-conductive tissue (with varying composition and morphology). It is, however, crucial that the plant is viable as dead tissue dehydrates inhibiting ionic conduction, which is essential for the energy conversion.^[6] Using living plants compared with artificial materials has several added benefits such as their dynamic self-repair and CO₂ compensation through ongoing growth which cannot be easily realized in artificial generators. Yet, the power outputs of plant-hybrid systems are limited and strategies to increase it are being developed. As contact electrification is a phenomenon

which is strongly dependent on the material pair in contact,^[36–39] the power output can be influenced by the materials that touch the plant.^[6] In addition, different plant species can result in different voltages generated.^[6] This enabled previous works to identify certain materials as well as plant species that lead to higher power outputs. Using silicone rubber, for example, generated voltages (up to 150 V for a 4.5 cm² leaf) and maximal power outputs of 0.15 W m⁻² leaf area under mechanical forces of 1 N were achieved on *Rhododendron* plants.^[6] Using *Magnolia denudata* and poly(methyl methacrylate), another research group obtained 0.045 W m⁻².^[28] A yet unexplored but crucial way to upscale the power output is using multiple leaves of a plant that act as individual generators interconnected via the plant tissue. In addition, how to exploit random and unpredictable environmental mechanical energy such as wind and related intricate plant leaf vibrations into electricity needs to be investigated.

Herein, we report the first proof-of-concept study on realization and design of whole living plant-based wind energy converters by analyzing the energy obtained from wind-induced vibrations between natural leaves and artificial silicone rubber leaves constrained to the petioles of the plant leaves (**Figure 1**). Two worldwide often found species, *Rhododendron yakushimanum* and *Nerium oleander*, have been modified for energy harvesting. The possibility to harvest energy by simultaneously gathering signals from up to eight leaves of the same plant was investigated under outdoor-relevant, yet highly controlled environments (such as wind speed, wind direction, humidity, light, and temperature).

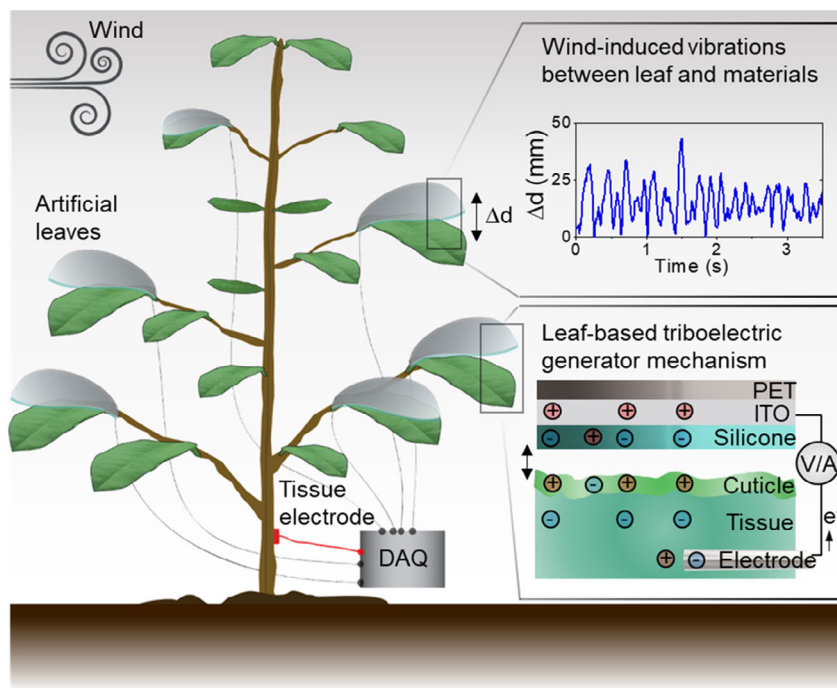


Figure 1. Illustration of the concept of living plant-hybrid systems that convert wind energy into electricity. Artificial (silicone rubber-based) leaves are installed at the plant and vibrate together with the natural leaves under wind excitation. This produces transient contacts between the leaves which generate surface charges on the plant and on the artificial leaf through contact electrification. These charges are induced into the inner plant tissue and into an electrode incorporated in the artificial leaves producing a current which is collected for data acquisition and energy harvesting.

The plants could harvest wind energy at different wind speeds and wind direction and moreover directly power light-emitting diodes (LEDs) and supply a digital thermal sensor. Our results point toward a realistic potential to upscale wind energy conversion using plants and this report suggests crucial design strategies to build plant-hybrid generators as standalone green power sources.

2. Results and Discussion

2.1. Concept of Multiple-Leaf Wind Energy Harvesting Using Living Plants

Figure 1 shows the concept exploited here for harvesting energy from plant-hybrid systems. The natural vibrations of leaves in the wind generate the mechanical energy that is converted into electricity. Contact electrification between plant leaves and artificial silicone rubber-based leaves installed at the plant forms surface charges that are induced into the tissue and in an electrode incorporated in the silicone rubber leaves, respectively.

Figure 2a shows the structure and dimensions of the artificial leaves [consisting of a silicone rubber-coated indium tin oxide (ITO) electrode on a polyethylene terephthalate (PET) support] that were installed at fully developed leaves by constraining them to the leaf petioles using a Velcro-based “plug-and-play”

attachment system that allows to easily change leaf positions and transfer to other plants (other fixations such as by tapes, threads, and glues may be used for permanent attachment). The artificial leaves are installed on top of the plant leaves and electrode materials have been chosen to be substantially transparent for light at wavelengths essential for plant’s photosynthesis (400–700 nm) to avoid affecting intrinsic physiological processes and being soft for avoiding damages of the plant tissue during mechanical impacts. Figure 2b–d shows the plant-hybrid generators after installation of the silicone leaves onto the test species. Both species (*R. yakushimanum* and *N. oleander*) have relatively hard and leathery (i.e., sclerophyllous) leaves as well as relatively robust petioles and stems which sustain the dynamic vibrations of the leaves together with the installed artificial leaves. Per plant, up to eight artificial leaves were connected, and Figure 2d,f shows the leaves which naturally differ slightly in size and shape. The leaves have been picked from the plants after finishing all tests and, notably, no damages were found due to the energy production (the holes in *R. yakushimanum* leaves are insect damages). Video 1, Supporting Information, shows a modified *R. yakushimanum* and *N. oleander* exposed to wind with turbulent flow dynamic in a dedicated phytochamber (described in Section 4 and Figure S1, Supporting Information). Video 2, Supporting Information, shows a slow-motion recording of the wind-induced vibrations of *R. yakushimanum* leaves and the flexible, transparent silicone leaves (hereafter called artificial

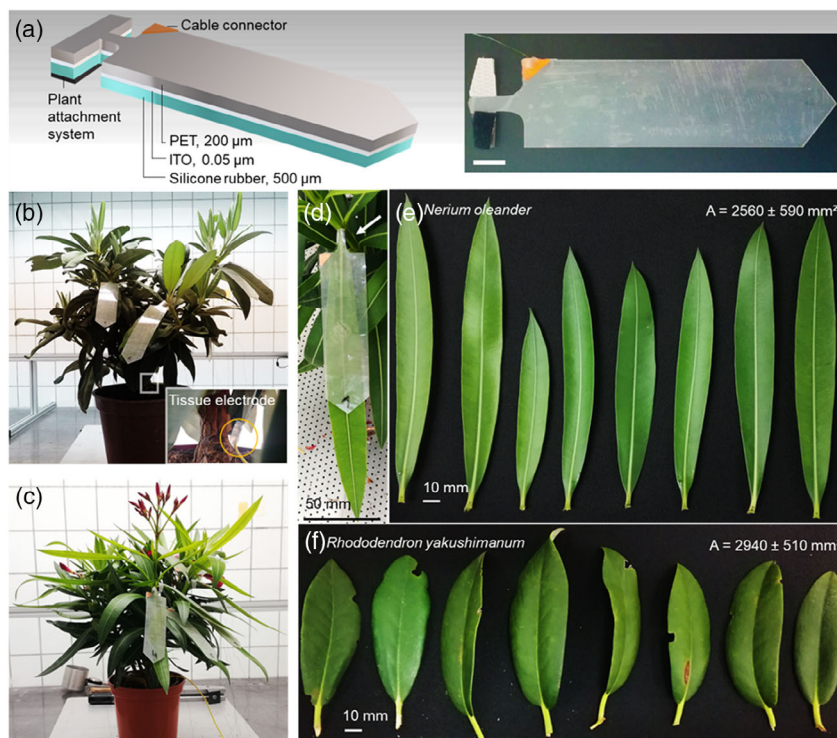


Figure 2. Structure of the artificial leaves and assembly of *R. yakushimanum* and *N. oleander* bushes as plant-hybrid wind energy harvesters. a) Illustration and image of the structure and dimensions of the artificial leaves used to enhance the energy output. b,c) Images of *R. yakushimanum* and *N. oleander*, respectively, with installed artificial leaves. The inset shows the tissue electrode in the trunk for harvesting the charges converted by the plant. d) Image of an *N. oleander* leaf with installed artificial leaf. The arrow points toward the petiole to which the artificial leaf is mechanically constrained. e,f) Images of the eighth leaves of *N. oleander* and *R. yakushimanum*, respectively, after being used for energy harvesting. No obvious damages are visible (the holes in *R. yakushimanum* leaves are damages caused by insects). The average surface area per leaf, A , is indicated.

leaves) at a wind speed of $4.2 \pm 0.2 \text{ m s}^{-1}$. Contact and separation between the leaf and the artificial leaf under wind excitation is the result of the different vibrational profiles of the two components. Leaf and artificial leaf are in still air only in contact at their fixation point at the petiole. The two layers are separated with an angle of $\approx 10^\circ\text{--}20^\circ$. Under wind excitation, both layers move with different amplitude and frequency leading to contact and separation (Video 2, Supporting Information). The initial angle between the two layers assists the mechanical separation which is required for the induction of charges into the tissue and the electrode, respectively. The amplitude Δd in Figure 1 describes the distance between two points, in the center of the leaf and the artificial leaf, respectively, illustrating a typical contact and release profile.

2.2. Wind-to-Electrical Energy Conversion by a Single Leaf

For testing the wind-to-electrical energy conversion, the modified plants were placed into a specialized phytochamber that enables to control wind speed, ambient humidity, temperature, and illumination during the experiments. Control over these parameters is essential for comparative measurements as they influence on

the one hand mechanical vibrations and contact electrification and on the other hand plant physiology. **Figure 3a** correlates the typical AC voltage time domains with the distance between the leaf and the mounted artificial leaf at a wind speed of $4.2 \pm 0.2 \text{ m s}^{-1}$. The voltage was measured at a tissue electrode in the trunk of the *R. yakushimanum* using the illustrated circuit. The correlation between the two curves confirms that the generated electricity is expectedly a function of contact and distance between the leaf and the silicone rubber. Both surfaces charge during each contact event generating the typical alternating current signal obtained by contact electrification-based triboelectric generators. Note that due to the established capacitor of charged leaf and artificial leaf, signals are also being produced when the leaves do not effectively touch but just vary their distance after a previous contact. This reduces mechanical impact on plant and artificial leaf while still enabling signal generation. Optimizing effective contacts of artificial triboelectric generators and wind generators has been considered as manner to reduce mechanical wear of materials involved and to maintain power output during long operation periods.^[40,41] Figure 3b shows the influence of wind and the artificial leaves on the output voltage signals by comparing the measurements without wind, with wind, and with

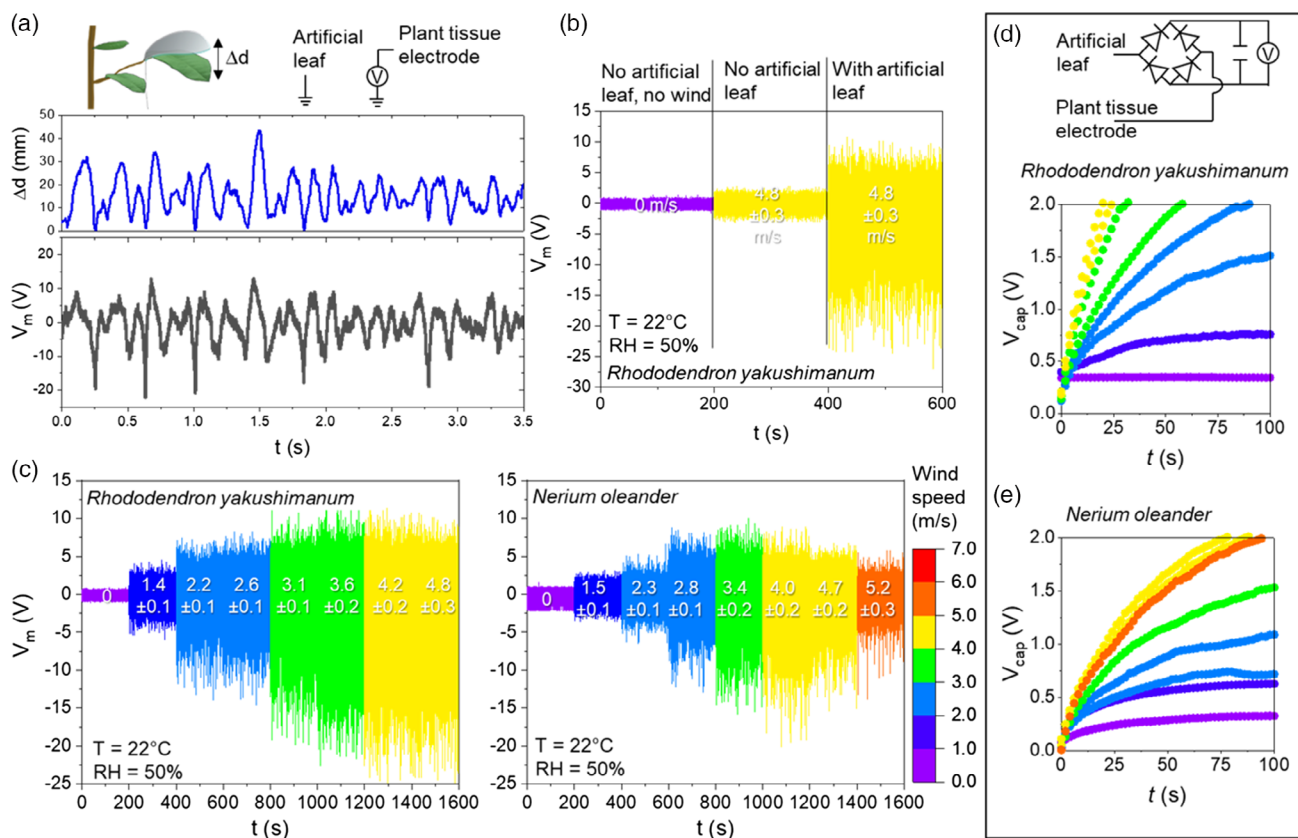


Figure 3. Wind-to-electricity conversion by plant-hybrid energy converters operating in single-leaf mode. a) Time domain open-circuit voltage V_m measured at the tissue electrode in the plant trunk using the indicated circuit and comparison with the vibrational profile in terms of distance variation Δd between an *R. yakushimanum* leaf and the artificial leaf at a wind speed of $4.2 \pm 0.2 \text{ m s}^{-1}$. b) V_m measured in the plant tissue with and without installed artificial leaf showing the enhancement of the output voltage. c) Influence of wind speed on V_m of a single *R. yakushimanum* and *N. oleander* leaf, respectively. d,e) Time-dependent voltage across a $0.333 \mu\text{F}$ capacitor V_{cap} which is charging by the plant-converted electricity using the indicated circuit at different wind speeds (colors indicate the wind speed according to the scale in part (c)) for *R. yakushimanum* and *N. oleander*, respectively. The points are averages of up to 30 charging cycles per wind speed; the standard deviations are smaller than the symbol sizes.

artificial leaves using the same circuit as shown in Figure 3a. The voltage signal significantly increases under wind excitation which is likely due to the plant leaf motion and self-contact between the leaves exposed to the wind. As expected, the voltage output is further improved when the artificial leaf is installed. This elevates the voltage amplitude to 33 ± 4 V at the same wind speed of 4.8 m s^{-1} which is about ≈ 10 times higher compared with the bare plant. In still air, a small environmental noise signal was present (see still air voltages in Figure 3c with different amplitudes of ≈ 1.6 and ≈ 3 V for *R. yakushimanum* and *N. oleander*, respectively, possibly related to the different internal resistances of the plants, $70 \text{ M}\Omega$ for *R. yakushimanum* and $184 \text{ M}\Omega$ for *N. oleander* as estimated from the capacitor charging curves given later). However, no noise filtering was applied, as the signal-to-noise ratio is high compared with those signals obtained under wind excitation (≈ 33 and ≈ 23 V amplitudes for *R. yakushimanum* and *N. oleander*, respectively). To test the wind speed dependency of the voltage generated, a hot wire anemometer was mounted close to the leaf under test and the voltage was measured while tuning the wind speed in the phytochamber from 0 until $\approx 6 \text{ m s}^{-1}$. This corresponds to characteristic surface winds on levels above ground at which plants grow.^[42] Figure 3c shows the relationship between the wind speed and the generated voltage showing a clear trend toward increased voltage outputs at higher wind speeds projected to be due to the increased vibrational amplitude, higher impact forces, and larger effective contact areas. The signal obtained from the *N. oleander* leaf also initially increases with higher wind speeds up to $4.0 \pm 0.2 \text{ m s}^{-1}$ and slightly reduces afterward. The reduction is likely because at higher wind speeds, the plant deforms and leaves turn (due to streamlining effects) which influences the vibration (see plant deformation as function of wind speed in Figure S2, Supporting Information). This behavior depends on the mechanical dynamics of the individual leaves and branches which can change as function of wind speed and individual plant structure.^[43] The generated signals were used to charge a capacitor ($0.333 \mu\text{F}$) using a simple rectifying circuit, and the voltage across the capacitors is shown in Figure 3d,e for *R. yakushimanum* and *N. oleander*, respectively, as a function of wind speed. The capacitor charging dynamics are expectedly wind-dependent and higher wind speeds prompt faster charging. The measurements confirm that energy conversion by the wind-induced vibrations and autonomous interaction of plants and installed materials is achieved and that the output is wind speed-dependent.

2.3. Multiple-Leaf Energy Harvesting and Scalability

Next, we tested if the overall energy output can be upscaled using multiple leaves of the same plant. This leads to a system in which signals generated from multiple leaves at different timings pass through the common tissue connection before being harvested at the electrode in the trunk. For the measurements, we installed eight artificial leaves on both *R. yakushimanum* and *N. oleander*, respectively, and used the signal acquisition circuit (Figure 4 and Figure S3, Supporting Information) that connects eight $0.333 \mu\text{F}$ capacitors to the eight artificial leaves and the trunk electrode. Each capacitor is hence fed by the common plant tissue electrode plus the electrode connected to each artificial leaf and the voltage

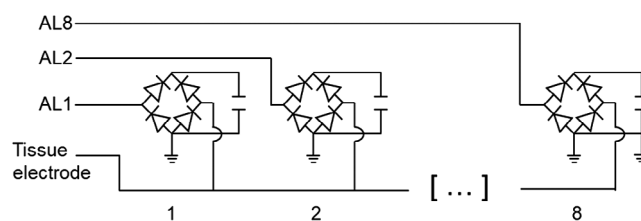


Figure 4. Basic elements of the data acquisition circuit for energy harvesting from eight leaves. AL1–8 indicate the individual electrodes connected with the artificial leaves. Further details and characteristics on the circuit are shown in Figure S3, Supporting Information.

across each capacitor is measured. The detailed description of the circuit and characteristics is given in Figure S3, Supporting Information.

Figure 5a,e shows the top-view images of the energy harvesting plants exposed to various wind speeds from two different directions (at 22°C and 50% relative humidity [RH]). The transferrable power was derived from $P_{\text{Cap}} = \frac{1}{2 \cdot t_1} \cdot C \cdot V_{\text{Cap}}^2$ and corrected by a factor taking circuit losses and internal resistance of the generator into account as shown in Figure S3, Supporting Information. C and V_{Cap} are the capacitance and the voltage across the capacitor, respectively; t_1 is the time interval required for charging the capacitor to 1 V. Figure 5c,d and f,g shows the obtained transferrable power P_{Cap} as function of the wind speed for *R. yakushimanum* and *N. oleander*, respectively. Note that the power output achieved under these conditions serves mainly for characterizing the multiple leaf harvesting and it is not the maximal achievable power output as discussed later. The data here are plotted against the individual wind velocities measured directly at the corresponding leaves. In this manner, the performance of each leaf can be compared. The output generally increases with the wind velocity whereas at still air, expectedly no power output was recorded. Some leaves perform significantly better than others as seen from the power outputs of individual leaves. Charge accumulation in the $0.333 \mu\text{F}$ capacitors starts at a wind speed of $\approx 2 \text{ m s}^{-1}$ indicating that the generated charges are now sufficient to compensate losses introduced by the circuit components leading to a positive power (Figure S3, Supporting Information, for further discussion). Figure 5e,h shows the sum power of all capacitors $P_S = \sum_{k=1}^{k=8} (P_{\text{cap}})_k$ for a given wind speed illustrating the additive energy obtained from the multiple leaves k . An interesting observation is made when considering the individual capacitor charging curves as shown in Figure 6a for *N. oleander* at a wind speed of $4.2 \pm 0.2 \text{ m s}^{-1}$ exemplary for a phenomenon seen in all tests. The graph shows that capacitors fed by leaves 1 and 7 reach highest voltage levels and charge faster than those connected with other leaves. In contrast, the individual capacitors connected to leaves 2–6 and 8 charge to lower voltages and all with nearly the same rates. The expected reason of the behavior is the following: leaves 1 and 7 perform best as they have likely the best orientation in the wind for obtaining the sufficient vibrational contact. By the circuit constraints, the artificial leaves 1 and 7 can only feed capacitors connected to these leaves and those charge faster. However, due to the common connection through the plant tissue, all charges produced by the plant are shared among all eight capacitors and charges

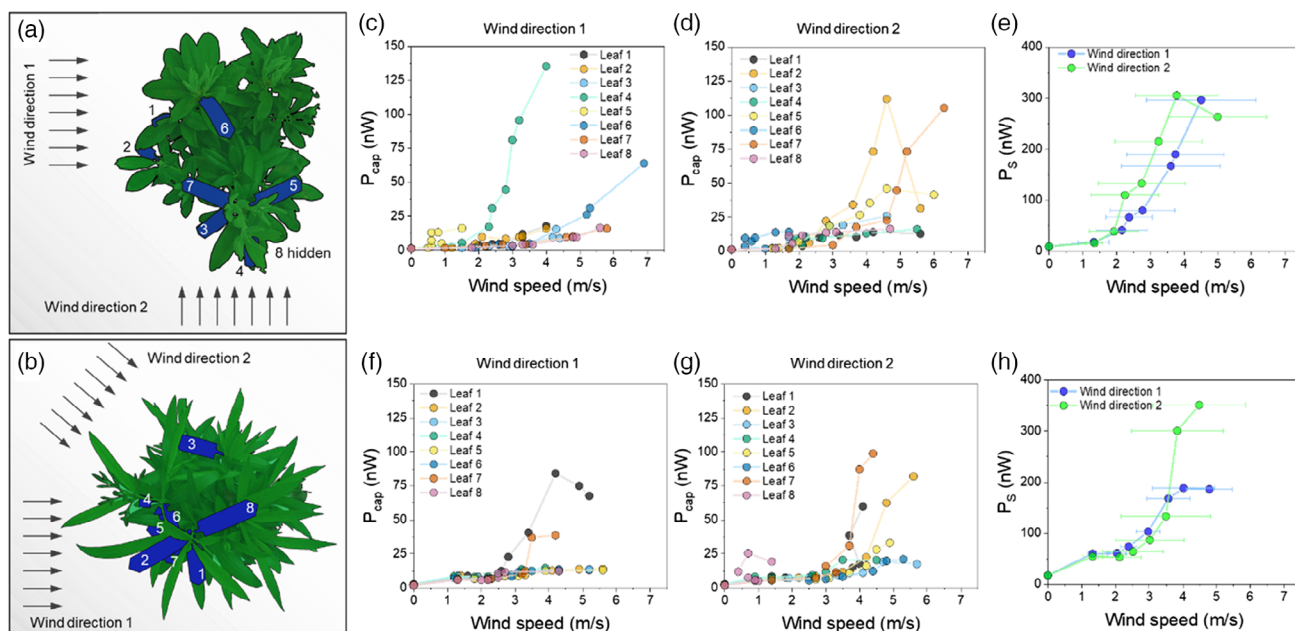


Figure 5. Multiple-leaf, multidirectional wind energy conversion. a, b) Top-view images of the *R. yakushimanum* and *N. oleander* plants, respectively, with eight installed artificial leaves highlighted in blue (colors changed for clarity). The arrows indicate the two wind directions investigated per plant. c, d) Plots of the power output P_{Cap} of *R. yakushimanum* obtained by analyzing the capacitor charging kinetics ($0.333 \mu\text{F}$) as a function of the wind speed and wind direction. e) Plots of the sum power P_s obtained by all eight *R. yakushimanum* leaves at a given wind velocity. f, g) Plots of the power output P_{Cap} of *N. oleander* as a function of the wind speed and the wind direction. e) Plots of the sum power P_s obtained by all eight *N. oleander* leaves. Standard deviations and error bars are obtained from up to 30 charging cycles per data point in parts (c)–(h) and they are smaller than the symbol size. Horizontal error bars in parts (e) and (h) represent the variation of the wind speed for the individual leaves.

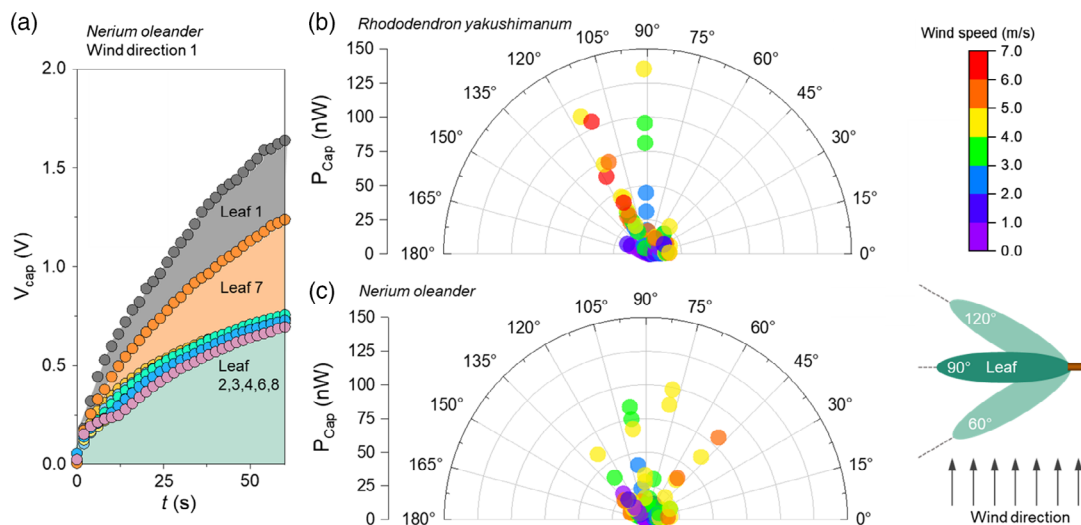


Figure 6. Influence of common tissue connection and impact of the wind direction on plant energy conversion. a) Representative charging rates of the individual $0.333 \mu\text{F}$ capacitors connected to the eight *N. oleander* leaves for wind direction 1 at a speed of $4.0 \pm 1.0 \text{ m s}^{-1}$. Leaves 1 and 7 are actively generating electricity and capacitors connected to these leaves are charging faster, whereas other capacitors are fed through charges shared through the common tissue connection. b, c) Polar plots illustrate the dependency of the stored energy on the wind direction and the wind speed indicating an optimum in near cross-flow orientation of the leaves with wind direction for both *R. yakushimanum* and *N. oleander*, respectively. The data points represent averages of up to 30 charging cycles and the standard deviations are smaller than symbol sizes.

produced at leaves 1 and 7, hence also feed the capacitors connected to leaves 2–6 and 8. The system compares with a network of interconnected triboelectric generators given by the fact that a

common connection is given via the plant tissue. Such parallelly coupled triboelectric generator networks have been suggested for large-scale wind and water wave energy harvesting in which

the power output is a sum of its individual generators.^[40,44–48] Notably, in our living plant-based system, it was not observed that the alternating signals (as, e.g., shown in Figure 2a) occurring from two or more leaves connected through the tissue cancel out as all capacitors accumulate charges. The fact that the positive and negative phases of the signals occur at irregular timings from random vibrational contacts and have short time domains (≈ 50 ms) renders an overlap an unlikely event. In addition, the differing ionic conduction paths for the individual leaves to the tissue electrode may play a role in the time domains and signal amplitudes. Overall, the positive power balance indicates that a single trunk electrode is sufficient at the given quantity of leaves but this aspect may need reconsideration in scenarios with much higher quantities of active leaves. The energy output is furthermore clearly influenced by the wind direction.

2.4. Wind Direction and Leaf Orientation

The results show that the pattern of which leaves actively convert energy changes when the wind direction changes. Figure 6b,c shows an analysis of power output in terms of the planar angles between leaves and the wind source as function of the wind speed for both *R. yakushmanum* and *N. oleander*, respectively. It can be observed that a near orthogonal orientation of leaves toward wind flow in angles spreading 90° – 120° for *R. yakushmanum* and 50° – 125° for *N. oleander* are working best. An optimal orientation can indeed be found at a cross-flow orientation of $\approx 90^\circ$ (*R. yakushmanum*) and $\approx 100^\circ$ (*N. oleander*) for which already wind speeds below 4 m s^{-1} lead to higher power compared with other leaf orientations at even higher wind speeds. Thus, an optimal orientation of leaves in the wind is crucial and information on the wind direction is a main parameter for concepting plant-hybrid energy harvesters in a natural environment. This behavior depends on the overall dynamics of the wind-induced motion which are species-dependent. Indeed, we observed differences among the two tested species expected to be related to the individual plant structure. For example, *R. yakushmanum* has an alternate leaf arrangement on the stem (spiral) and for *N. oleander* several leaves arise from the same level (whorled leaf arrangement) that likely prompts a different motion of the leaves in the wind. Other properties, such as the leaf size, the shape, the weight, the branch motion, and hence the overall plant biomechanics will influence the wind direction dependency of the fluttering and energy output.

In a potential outdoor application situation, several factors next to wind speed and direction play additional roles. Crucial impact has the humidity as it is known to influence contact electrification. The impact of the ambient humidity on the voltage generation was tested by regulating RH in the phytochamber from $\approx 30\%$ to 70% while maintaining a constant wind speed (Figure S4, Supporting Information). The measured voltage amplitudes decrease from ≈ 40 to ≈ 20 V when shifting RH from 30% to 70% . However, we found that the process is reversible: reducing RH in turn to lower values recovers the originally generated voltage amplitudes. It follows that a humid or rainy day will decrease, whereas a dry day will increase the energy output.

2.5. Applications, Overall Perspective, and Energy Output

The results reveal first essential design strategies for plant-based wind energy converters that transduce wind-induced vibrations of multiple leaves into electricity in a wind speed and wind-direction-dependent manner. Indeed, such configurations can be used to directly power LEDs by plant's motion in the wind as shown in Video 3, Supporting Information. Moreover, the energy when accumulated for certain periods can power sensors. Figure S5 and Video 4 and 5, Supporting Information, show a digital thermometer that is powered by *N. oleander*. In a configuration with controlled stimulation at an impact force of 0.8 N applied on the plant by an actuator, it required about 8 min to charge a $50 \mu\text{F}$ capacitor to 1.5 V . With four artificial leaves during exposure to wind of a speed of $\approx 3 \text{ m s}^{-1}$, the capacitor charges to 1.5 V in only ≈ 15 min providing enough energy for driving the thermal sensor and powering the sensing circuit, including the display showing the reading. This indicates that even few leaves are sufficient to perform a sensing task in a duty cycled circuit, more leaves will provide more energy pointing toward many potential applications. The fact that the energy scales with wind speed and wind directions suggests, moreover, the opportunity to use the plant as wind sensors. Due to the novelty and interdisciplinarity of the research, the discussion on an overall perspective of the technology for energy harvesting begins with a survey of which factors will require further investigation in future to create reliable plant-hybrid wind energy converters. Many fundamental aspects require thorough investigation, including the phenomena of contact electrification on plant surfaces, the optimization of the materials used, and the processes occurring in the biological organism. Our plant-based triboelectric generators operate mainly in vertical contact mode; other potential operational modes may also include sliding-mode triboelectric electrification in which the leaf or a whole branch with several leaves slide over an artificial surface driven by the wind. In any operational mode, it is essential how adapting artificial components to certain plant species for tailoring the energy conversion efficiency while maintaining plant survival. The latter is essential for the robustness of the generators and the long-term reliability. An advantage over completely artificial systems is that plants have some “built-in” processes which can assist long-term functionality such as self-repair of the cuticle, and many plants have self-cleaning properties. Certainly, the mechanical impact produced by the artificial leaf should neither be destructive nor should inhibit plant growth. We thus used soft (silicone rubber) artificial leaves to reduce mechanical wear and damage of the leaf, and we indeed did not observe any wind-induced damages of the leaves in any case. Transparent electrodes that let light pass for processes such as photosynthesis are essential and also other environmental effects such as humidity need to be considered. Our electrodes are fully sealed with silicone rubber (and PET on top), and the results show that power output can restore when humidity reduces. Very high humidity and rain could be exploited as benefit for cleaning the artificial leaves from, e.g., dust and hence help to sustain the system, but further investigations are required to evaluate the complex influence of environmental parameters in an outdoor study. As mentioned before, tailoring the number of contacts can be optimized toward

reduction of mechanical wear.^[41] However, from time to time contact between leaf and artificial leaf is necessary for charging the surfaces; once charged, the motions of the leaf and artificial leaf alone also generate electricity due to the varying capacitor. It hence needs to be studied how long charges remain on the leaf surface and how to tailor the mechanics of the system. Adapting the artificial leaf toward a certain plant species such as by tailoring its natural frequency can be an option to control vibrational profiles. In addition, the fixation and initial angle may be tailored such as that the angle is not too large so that the wind excitation might not be sufficient to bring both surfaces together and at the same time not too small to assist the charge separation.

Another aspect is the overall energy conversion and storage efficiency which is also a communal challenge of many artificial energy harvesters such as triboelectric nanogenerators. Electronic circuits need to be developed that can handle the random input signals with arbitrary frequencies from multiple sites. The maximal power is then dependent on multiple factors such as frequency, forces, effective contact area, internal resistances, ionic paths in the tissue, the energy storage, e.g., the capacitance, the efficiency of contact electrification which requires adaptation for plant-hybrid systems. Indeed, the power analysis that we report here does not contain any optimized circuitry and serves only the purpose to study the basic capability of the plant-hybrid energy converters. Other circuits may further improve the power output such as by, e.g., considering groups of leaves with synchronized movements (e.g., those which have a similar orientation to wind direction). The potential for increasing the power output is given by tailoring these diverse factors. In addition, we studied maximal eight “generator-leaves” per plant. This number can be increased and larger plants which may have thousand to ten thousand of leaves will gather significantly more energy. This raises a question on how to wire large amounts of natural and artificial leaves, or if instead the artificial leaves could also share common connections. Indeed, the circuit by the plants, its internal impedances, and ionic conduction paths need to be investigated among other mentioned aspects. Although many issues still need to be resolved in future, this work proves the possibility and potential for using plants as scalable wind energy converters.

3. Conclusion

Our study gives a clear evidence that plant-hybrid generators have the potential to convert wind energy into electricity in a scalable manner for lighting or powering sensors. Wind is first converted by the plant into a mechanical energy and then transduced into electricity using the wind-induced vibrations and contacts between plant leaves, enhanced by artificial leaves of tailored materials installed at the leaves. The signals from contact electrification and induction by multiple leaves can be simply harvested by a common electrode in the plant tissue. The power output scales with the wind speed and adds up with the amount of leaves that actively convert energy depending on the leaf orientations with an optimum at cross-flow orientation regarding wind direction at the given system designs. Up to 50 LEDs and a digital thermal sensor including display could be powered by an *N. oleander* plant with only four artificial leaves. Further

improvements by developing the materials, mechanical dynamics, and energy harvesting electronics will enable off-grid plant-based and literally green generators that will find application in sensing, environmental monitoring, lighting, and other tasks.

4. Experimental Section

Plant Species: An *R. yakushmanum* bush (height 39 cm, diameter 55 cm) and an *N. oleander* bush (height 28 cm, diameter 42 cm) were provided by the Botanic Garden, University of Freiburg, Germany. The plants were daily watered and kept in a phytochamber with lighting in a 16 h day and 8 h night cycle.

Fabrication of Artificial Leaves for Plant-Hybrid Generators: Transparent ITO-coated PET films (thickness 200 μm, nominal sheet resistance 350–500 Ω square⁻¹) were purchased from Thorlabs Inc., USA. A thin layer of silicone rubber adhesive (Sil-Poxy, Smooth-On Inc., USA) was applied on the ITO layer using a doctor blade. Subsequently, a layer of translucent silicone rubber was added (thickness 500 μm, obtained from Modulor GmbH, Germany, which was previously washed with isopropyl alcohol and dry wiped using dust-free tissue). The layers were dried for a minimum of 24 h before they were cut into the desired shapes using a laser cutter (VersaLaser VLS3.60, Universal Laser Systems Inc., USA). Self-adhesive Velcro strips were glued onto the two wings of the lower end of the artificial leaf (Figure 2a) as an attachment system to fix the artificial leaves onto the plant's petioles. In addition, to connect the ITO electrode, the silicone film was carefully lifted from the ITO electrode in one corner and a piece of copper tape with conductive glue was attached to the ITO layer. Then, the cable was soldered onto the copper tape and the silicone layer was brought back and fixed using the silicone adhesive. All cutting edges were sealed with silicone. The leaves were attached onto the petioles of the natural leaves for energy conversion and further analysis.

Phytochamber and Wind Source: The exposure of the plant-hybrid energy harvesters to winds of controllable speed different environments (humidity, temperature, and light) was performed in a specialized phytochamber (height: 2.13 m, depth: 2.75 m, width: 2.5 m) equipped with an active climate control system and a wind source consisting of 96 individually adjustable nozzles (Figure S1, Supporting Information) that were all oriented toward the plant which was placed in a distance of ≈50 cm from the nozzles (measured from the plant center). A ventilation system (MUB 042-500DV-A2, Systemair, Skinnskatteberg, Sweden [max speed: 1330 rpm]) in combination with a frequency converter (VLT HVAC Drive FC 102, Danfoss, Nordborg, Denmark) allowed controlling the wind speed. Each time a wind speed was set, the actual wind speed at the individual leaves under analysis was measured at a distance of ≈3 cm in front of the leaf using a hot wire anemometer (405i, Testo SE & Co. KGaA, Germany) as the actual wind speed affecting the leaves may differ due to varying distances from the wind source, shading of other plant parts, and different leaf orientations. During all measurements, illumination was kept constant and the temperature was kept at 22 ± 1 °C. The RH was typically 50 ± 3% or varied between 30% and 70% RH as indicated in the figures. Temperature and humidity were continuously monitored using a humidity and temperature data logger (EL-USB-2+, Lascar Electronics Ltd., Whiteparish, UK).

Data Acquisition: Voltages in single-leaf experiments were measured with an oscilloscope (MSO7014A, Agilent Technologies, USA). Short-circuit currents were measured using a high input impedance electrometer (6517B, Keithley, USA). To simultaneously record signals from eight leaves, a data acquisition circuit (Figure 4 and Figure S3, Supporting Information) was designed in which eight individual ceramic capacitors (0.333 μF obtained by three serial 1 μF capacitors, 16 V, Taiyo Yuden Co. Ltd., Japan) were charged by the generated signals after rectification. The circuit automatically measures the voltage across the capacitors and discharges the capacitors when a certain set threshold voltage (typically 2 V in our experiments) is reached. The circuit was tested in detail before the analysis, and further details and characteristics are

given in Figure S3, Supporting Information. The voltage across the capacitors was tracked at a frequency of 1 Hz for typically 10 min and up to 33 charging cycles occurred during this time depending on the wind speed and other factors such as leaf orientation. The average and standard deviations (typically smaller than the symbol sizes in the graphs) are given.

Supporting Information

Supporting Information is available from the Wiley Online Library or from the author.

Acknowledgements

This work was funded by the project GrowBot, the European Union's Horizon 2020 Research and Innovation Programme under grant agreement no. 824074. T.S. acknowledges additional funding by the German Research Foundation (Deutsche Forschungsgemeinschaft, DFG) under Germany's Excellence Strategy—EXC-2193/1-390951807.

Conflict of Interest

The authors declare no conflict of interest.

Keywords

bioelectronics, bioinspiration, plants, triboelectric generators, wind energy harvesting

Received: March 12, 2020

Revised: April 15, 2020

Published online: May 12, 2020

- [1] W. Jiang, H. Li, Z. Liu, Z. Li, J. Tian, B. Shi, Y. Zou, H. Ouyang, C. Zhao, L. Zhao, R. Sun, H. Zheng, Y. Fan, Z. L. Wang, Z. Li, *Adv. Mater.* **2018**, *30*, 1801895.
- [2] P. Tan, Q. Zheng, Y. Zou, B. Shi, D. Jiang, X. Qu, H. Ouyang, C. Zhao, Y. Cao, Y. Fan, Z. L. Wang, Z. Li, *Adv. Mater.* **2019**, *9*, 1901875.
- [3] Y. Zou, P. Tan, B. Shi, H. Ouyang, D. Jiang, Z. Liu, H. Li, M. Yu, C. Wang, X. Qu, L. Zhao, Y. Fan, Z. L. Wang, Z. Li, *Nat. Commun.* **2019**, *10*, 2695.
- [4] J. Sun, A. Yang, C. Zhao, F. Liu, Z. Li, *Sci. Bull.* **2019**, *64*, 1336.
- [5] H. Ouyang, Z. Liu, N. Li, B. Shi, Y. Zou, F. Xie, Y. Ma, Z. Li, H. Li, X. Qu, Y. Fan, Z. L. Wang, H. Zhang, Z. Li, *Nat. Commun.* **2019**, *10*, 1821.
- [6] F. Meder, I. Must, A. Sadeghi, A. Mondini, C. Filippeschi, L. Beccai, V. Mattoli, P. Pingue, B. Mazzolai, *Adv. Funct. Mater.* **2018**, *28*, 1806689.
- [7] O. Speck, T. Speck, *Biomimetics* **2019**, *4*, 26.
- [8] W. Barthlott, M. Mail, B. Bhushan, K. Koch, *Nano-Micro Lett.* **2017**, *9*, 1.
- [9] B. Mazzolai, L. Beccai, V. Mattoli, *Front. Bioeng. Biotechnol.* **2014**, *2*, 1.
- [10] E. Environ, A. A. Boghossian, M. Ham, H. Choi, M. S. Strano, *Energy Environ. Sci.* **2011**, *4*, 3834.
- [11] J. P. Giraldo, H. Wu, G. M. Newkirk, S. Kruss, *Nat. Nanotechnol.* **2019**, *14*, 541.
- [12] M. H. Wong, J. P. Giraldo, S. Y. Kwak, V. B. Koman, R. Sinclair, T. T. S. Lew, G. Bisker, P. Liu, M. S. Strano, *Nat. Mater.* **2017**, *16*, 264.
- [13] S.-Y. Kwak, J. P. Giraldo, M. H. Wong, V. B. Koman, T. T. S. Lew, J. Ell, M. C. Weidman, R. M. Sinclair, M. P. Landry, W. A. Tisdale, M. S. Strano, *Nano Lett.* **2017**, *17*, 7951.
- [14] R. Di Giacomo, C. Daraio, B. Maresca, *Proc. Natl. Acad. Sci.* **2015**, *112*, 4541.
- [15] J. J. Kim, L. K. Allison, T. L. Andrew, *Sci. Adv.* **2019**, *5*, eaaw0463.
- [16] E. Stavrinidou, R. Gabrielsson, E. Gomez, X. Crispin, O. Nilsson, D. T. Simon, M. Berggren, *Sci. Adv.* **2015**, *1*, e1501136.
- [17] E. Stavrinidou, R. Gabrielsson, K. P. R. Nilsson, S. K. Singh, J. F. Franco-Gonzalez, A. V. Volkov, M. P. Jonsson, A. Grimoldi, M. Elgland, I. V. Zozoulenko, D. T. Simon, M. Berggren, *Proc. Natl. Acad. Sci.* **2017**, *114*, 2807.
- [18] T. T. S. Lew, V. B. Koman, P. Gordiichuk, M. Park, M. S. Strano, *Adv. Mater. Technol.* **2019**, *5*, 1900657.
- [19] R. Nitisoravut, R. Regmi, *Renewable Sustainable Energy Rev.* **2017**, *76*, 81.
- [20] D. P. B. T. B. Strik, R. A. Timmers, M. Helder, K. J. J. Steinbusch, H. V. M. Hamelers, C. J. N. Buisman, *Trends Biotechnol.* **2011**, *29*, 41.
- [21] D. P. B. T. B. Strik, H. V. M. H. Bert, J. F. H. Snel, C. J. N. Buisman, *Int. J. Energy Res.* **2008**, *32*, 870.
- [22] H. Deng, Z. Chen, F. Zhao, *ChemSusChem* **2012**, *5*, 1006.
- [23] A. J. McCormick, P. Bombelli, R. W. Bradley, R. Thorne, T. Wenzel, C. J. Howe, *Energy Environ. Sci.* **2015**, *8*, 1092.
- [24] A. Mershin, K. Matsumoto, L. Kaiser, D. Yu, M. Vaughn, K. Nazeeruddin, B. D. Bruce, M. Graetzel, S. Zhang, *Sci. Rep.* **2012**, *2*, 234.
- [25] J. Tschörtner, B. Lai, J. O. Krömer, *Front. Microbiol.* **2019**, *10*, 866.
- [26] V. Flexer, N. Mano, *Anal. Chem.* **2010**, *82*, 1444.
- [27] T. Miyake, K. Haneda, N. Nagai, Y. Yatagawa, H. Onami, S. Yoshino, T. Abec, M. Nishizawa, *Energy Environ. Sci.* **2011**, *4*, 5008.
- [28] Y. Jie, X. Jia, J. Zou, Y. Chen, N. Wang, Z. L. Wang, X. Cao, *Adv. Energy Mater.* **2018**, *8*, 1703133.
- [29] D. W. Kim, S. Kim, U. Jeong, *Adv. Mater.* **2018**, *30*, 1804949.
- [30] D. Choi, D. W. Kim, D. Yoo, K. J. Cha, M. La, D. S. Kim, *Nano Energy* **2017**, *36*, 250.
- [31] M. Riederer, C. Müller, *Biology of the Plant Cuticle* (Eds: M. Riederer, C. Müller), Blackwell Publishing Ltd Editorial, Oxford, UK **2006**.
- [32] C. Wu, A. C. Wang, W. Ding, H. Guo, Z. L. Wang, *Adv. Energy Mater.* **2019**, *9*, 1802906.
- [33] Z. L. Wang, *ACS Energy Lett.* **2013**, *7*, 9533.
- [34] Z. L. Wang, J. Chen, L. Lin, *Energy Environ. Sci.* **2015**, *8*, 2250.
- [35] M. Wong, W. Xu, J. Hao, *Adv. Funct. Mater.* **2019**, *29*, 1904090.
- [36] J. Lowell, A. C. Rose-Innes, *Adv. Phys.* **1980**, *296*, 947.
- [37] D. J. Lacks, T. Shinbrot, *Nat. Rev. Chem.* **2019**, *3*, 465.
- [38] L. S. Mccarty, A. Winkleman, G. M. Whitesides, *J. Am. Chem. Soc.* **2007**, *129*, 4075.
- [39] F. Galembeck, T. A. L. Burgo, *Chemical Electrostatics*, Springer International Publishing, Cham **2017**.
- [40] L. Huang, W. Xu, G. Bai, M. Wong, Z. Yang, J. Hao, *Nano Energy* **2016**, *30*, 36.
- [41] W. Xu, M. Wong, J. Hao, *Nano Energy* **2019**, *55*, 203.
- [42] Z. Jiao-jun, L. Xiu-fen, G. Yutaka, M. Takeshi, *J. For. Res.* **2004**, *15*, 305.
- [43] X. Amandolese, M. Saudreau, P. He, T. Leclercq, E. De Langre, *J. R. Soc. Interface* **2018**, *15*, 20180010.
- [44] A. Ahmed, I. Hassan, M. F. El-kady, A. Radhi, C. K. Jeong, P. R. Selvaganapathy, J. Zu, S. Ren, Q. Wang, R. B. Kaner, *Adv. Sci.* **2019**, *6*, 1802230.
- [45] A. Ahmed, I. Hassan, M. Hedaya, T. A. El-yazid, J. Zu, Z. Lin, *Nano Energy* **2017**, *36*, 21.
- [46] L. Xu, T. Jiang, P. Lin, J. J. Shao, C. He, W. Zhong, X. Y. Chen, Z. L. Wang, *ACS Nano* **2018**, *12*, 1849.
- [47] X. Yang, L. Xu, P. Lin, W. Zhong, Y. Bai, J. Luo, J. Chen, *Nano Energy* **2019**, *60*, 404.
- [48] M. Gordel, R. Kolkowski, J. Olesiak-Banska, K. Matczyszyn, M. Buckle, M. Samoć, *J. Nanophotonics* **2015**, *9*, 093797.